ICE STAGNATION IN PLEISTOCENE VALLEY GLACIERS, SAN JUAN MOUNTAINS, COLORADO: DEPOSITS AND A MODEL OF CONTROLS

Eric E. Small
Department of Geology
Williams College
Williamstown, MA 01267

INTRODUCTION

This study has two goals:

1) To describe and interpret Pleistocene valley glacier stagnant ice deposits in the San Juan Mountains, Colorado. Stagnant ice retreat and resulting deposits have not been recognized by previous workers in ancient valley glacier settings. Dead ice indicators are abundant in the San Juan Mountains and can be used to understand this process in Pleistocene valley glacier systems.

2) To determine the controls of ice stagnation in valley glacier systems. Controls of this process are not presently understood. Previous workers have suggested possible causes of stagnation for single glaciers; however, no earlier studies have determined what mix of variables is responsible for inducing this process in general. In an attempt to understand the controls of this process, a model of ice stagnation is developed in this study and tested with data from fifty valleys in the San Juans.

The San Juan Mountains are located in southwestern Colorado. Ice covered 5000km^2 of the San Juans during the most recent glacial maximum. Other than two large icefields, which formed over the high mountains and buried the continental divide, most of the Pleistocene ice in the San Juans were valley glaciers(Atwood and Mather, 1932). Detailed field work was completed in the eastern San Juans near Creede, Colorado; 107°00'W longitude and 37°40'N latitude. The middle fork of Roaring Creek, Red Mountain Creek and South Clear Creek were studied in detail. Aerial Photos from the entire San Juans range were examined.

STAGNANT ICE FEATURES

Topography

Areas of stagnant ice topography were examined using total station, plane table and alidade, and tape and inclinometer. A map of this topography in Roaring Creek valley was produced using plane table and alidade (Figure 1). This area is characterized by chaotic hummocks (kames), closed boggy depressions (kettles) and two sinuous, valley parallel ridges (eskers). This stagnant ice complex is surrounded by linear, sharp lateral, recessional and terminal moraines indicating deposition by active ice processes. Average maximum slope angle and mean slope angle of profiles across the stagnant and active ice areas demonstrate that different processes are responsible for construction of landforms (Figure 1). Previous workers have described deposits similar to these stagnant ice deposits in other areas of the San Juans.

Sedimentology

Sedimentological characteristics of ice stagnation complexes were investigated by completing measured sections, photographing outcrops, measuring fabric and analyzing sediment grain size and texture. The following sedimentological signatures of stagnant ice deposition were found: (1) extreme lateral and vertical variability in grain size, sorting and sedimentary structures indicating spatial and temporal heterogeneity in depositional processes (figure 2a); (2) patterns of esker sedimentation including interbedded fluvial gravels and quiet water deposits, and higher energy processes at the center of esker-shaped landforms (Figures 2b and 2c); and (3) faulted and tilted bedding from melting of supporting or buried ice blocks (Flint, 1971). These characteristics, along with facies associations, fabric data and spatial and temporal changes in sedimentation patterns, confirm that stagnant ice depositional processes were active in Pleistocene valley glaciers in the San Juans.

Aerial Photo Survey

Examination of aerial photos of 80 glaciated valleys in the San Juans indicates that stagnant ice topography is present throughout the entire San Juan range. Of the valleys studied, one third exhibited clear stagnant ice topography while another third were completely free of this indicator. It was not apparent whether ice stagnation occurred in the remaining valleys. Ice stagnation zones are most frequently 500m long and 200-300m wide with long axes parallel to the valley. These zones are usually limited to a single location in each valley.

ICE STAGNATION MODEL

A model was constructed, based on empirical and theoretical laws of glacier flow, to determine whether a receding valley glacier will develop a stagnant or an active margin. According to this model, ice stagnation can occur in two ways: (1) a topographic feature thins the glacier to a critical thickness, retarding internal deformation and pinching off a section of unnourished ice downstream (Figure 3a) and (2) downward melting can be slower than retreat of the active ice margin, the climatically controlled downstream limit to which ice flows, also stranding

Table 2. Results of paleohydraulic calculations.

Method	Cross-Section CS	Average Depth (m) D	Average Velocity (ms^{-1}) v	Discharge (m^3s^{-1}) Q	Average Discharge (m^3s^{-1}) of both cross-sections
Baker (1974) (dimensionless shear stress=0.06)	CS3	11.6	9.9	137,860.9	94,056.7
	CS4	12.3	10.0	50,252.5	
Baker (1974) (dimensionless shear stress=0.02)	CS3	3.9	3.9	6,374.0	6,954.7
	CS4	4.1	4.0	7,535.4	
Williams (1983)	CS3	3.0	2.6	2,480.8	2,166.4
	CS4	3.2	2.6	1,851.9	
Costa (1983)	CS3	4.6	5.7	9,773.0	7,277.3
	CS4	4.9	5.7	4,781.5	

Post-Glacial Deposition

Most of the valley is covered with post-glacial landforms formed by erosion of the northeast valley wall (Figure 2). The largest feature is the 4 km^2 landslide utilized as a dam for the Santa Maria Reservoir (LS1). It is indicated by hummocky topography with closed depressions and debris clasts up to 10 m in diameter. Other smaller slides, LS2 and LS3 also originate from the northeast canyon wall. LS2 occurred as three separate events distinguishable by differences in soil and vegetation cover. Sharp-edged rock clasts with little soil or vegetation form the youngest slide, LS2c. The middle slide, LS2b, has some soil, grass, and tree cover, and the toe of the oldest slide, LS2c, remains as a hummocky, silt-covered mound beneath the other two slides.

Alluvial fans with active debris flows are also transporting sediment to the valley floor. AF1 is the largest fan transporting sediment from the scarp of LS1 and burying parts of the slide's SE end. Gullies form the head of Seepage Creek and transport sediment and water carried by debris flows, by piping through the old slide, and by overland wash. Some are 300 cm deep and reveal a thick sequence of valley fill dominated by silt.

A radiocarbon date from the dry lake bed of Ghost Lake indicates that LS1 occurred before 7,610 +/- 90 yr B.P.. The lake lacks an outlet or inlet and was fed by seepage through the landslide. No channels cut through the slide or the deposits on the valley floor, indicating that LS1 and most of the valley's geomorphic features were deposited after the flood.

Conclusion

Evidence in the Santa Maria Canyon indicates glaciation, followed by flooding, followed by hillslope erosion. First, ice from the Rio Grande Glacier flowed into the canyon. Between 16,380 and 13,500 yr B.P. Glacial Lake Atwood drained catastrophically through the Santa Maria Canyon, with a discharge between 2166 m^3s^{-1} and 7277 m^3s^{-1} forming channels and depositing boulders. Since flooding, hillslope erosion has shaped the valley, a major event occurring before 7,610 =/-90 yr B.P., when part of Bristol Head tumbled to the canyon floor and formed the LS1 deposit.

References Cited

Atwood W.W. and Mather K.F., 1932, Physiography and Quaternary geology of the San Juan Mountains, Colorado: U.S. Geological Survey Professional Paper 166. 176p.

Baker, V.R., 1974, Paleohydraulic interpretation of Quaternary alluvium near Golden, Colorado: Quaternary Research, v.4, p.94-112.

Carson, R., personal communication, 1992.

Colman, S.M. and Pierce, K.L., 1981, Weathering rinds of basaltic and andesitic stones as Quaternary age indicator western U.S.: U.S. Geological Survey Professional Paper 1210.

Costa, J.E., 1983, Paleohydraulic reconstruction of flash-flood peaks from boulder deposits in the Colorado Front Range, Geological Society of America Bulletin, v.94, p.986-1004.

Elias, S.A., Carrara, P.E., Toolin, L.J., and Jull, J.T., 1991, Revised age of deglaciation of Lake Emma based on new radiocarbon and macrofossil analyses: Quaternary Research, v.36, p.307-321.

Kitchens, S., this volume.

MacGregor, K., this volume, Late Pleistocene history of Glacial Lake Atwood, San Juan Mountains, Colorado.

Madole, R.F., 1986, Lake Devlin and Pinedale glacial history, Front Range, Colorado: Quaternary Research, v.25, p.43-54.

McMillan, S., this volume, Late Pleistocene deglaciation of the Clear Creek Graben, San Juan Mountains, Colorado.

Porter, S.C., Pierce, K.L., Hamilton, T.D., 1983, Late Wisconsin mountain glaciation in the western United States, *in* Porter, S.C., ed., Late Quaternary Environments of the United States: Vol. 1: The Late Pleistocene: Minneapolis, University of Minnesota Press, p.71-110.

U.S. Department of Agriculture, 1985, Aerial Photographs 684-177 -179 and 684-153 -155.

U.S. Geological Survey, 1964, Workman Creek Quadrangle, Colorado: 7.5 Series (Topographic), DMA 4559 II NE-Series V877. scale 1:24,000.

U.S. Geological Survey, 1986, Bristol Head Quadrangle, Colorado: 7.5 Series (Topographic), DMA 4559 I SE-Series V877. scale 1:24,000.

Williams, G.P., 1983, Paleohydrological methods and some examples from swedish fluvial environments: I Cobble and boulder deposits: Geografiska Annaler, 65 A (3-4), p.227-243.

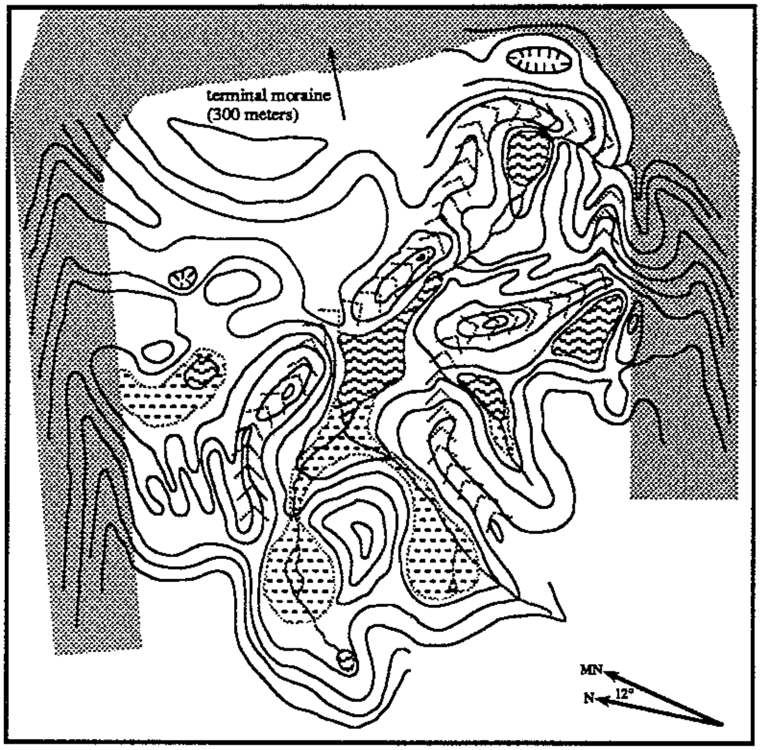

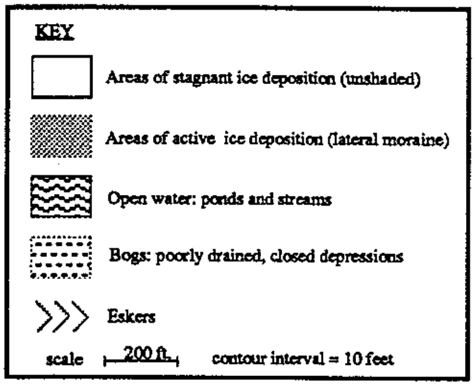

Type of deposition	Avg. max. slope angle	Mean slope angle
Active ice	24.8 ± 1.4	13.1±1.5
Stagnant ice	16.5 ± 1.7	7.3 ± .4

Figure 1. Plane table and alidade map of the Roaring Creek ice stagnation zone. This ice stagnation zone is surrounded by an area of active ice depostion (shaded). Comparison of slope angles between the stagnant and active ice areas is made in the box on the bottom right.

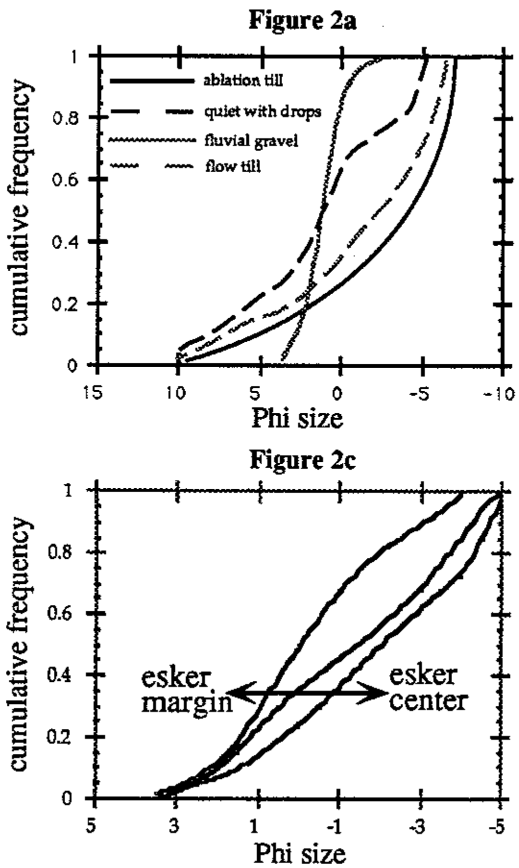

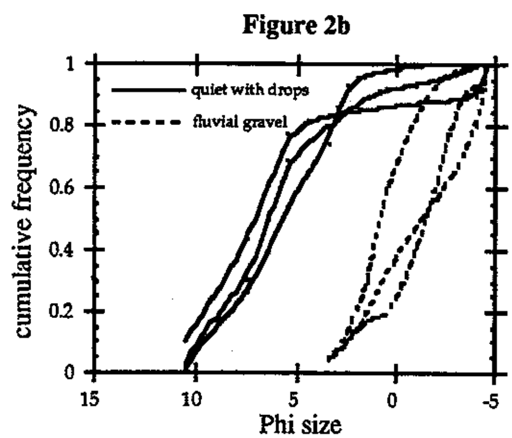

Figure 2. Cumulative frequency grain size graphs demonstrating signatures of stagnant ice deposition: **2a)** varied depositional processes represented on a single kame; **2b)** interbedded fluvial gravels and quiet water deposits with dropstones. Different lines represent several sites along the northern esker; 2c) moderatly sorted fluvial gravels indicating stronger flow at the center of the esker and weaker flow at margins. Lines represent a single cross-section through the southern esker.

unnourished ice (Figure 3b). Different variables cause stagnation in these two scenarios. Determination of what variables are the most important controls of ice stagnation will be achieved by applying data from the 50 valleys studied in the aerial photo survey to this model. The model uses the following information from each valley: (1) bedrock profile; (2) valley width at all points; and (3) slope angle and aspect.

Stagnation from Critical Thickness

The flow law for ice (Glen, 1952) indicates that ice will not internally deform when shear stress is below approximately 50kPa. Shear stress at the base of a glacier can be approximated by the following equation (Nye, 1965):

$$\tau = \rho g h (\sin\alpha) F \qquad \text{(eqn. 1)}$$

where τ is shear stress, ρ is the density of ice (910 Kg m^{-3}), g is acceleration due to gravity (9.81 m s^{-2}), h is the thickness of the glacier, α is the angle of the ice surface and F is a shape factor which takes into account the width and cross-sectional shape of the valley. Rewriting this equation for the boundary condition where internal deformation stops (τ = 50kPa), we can determine the critical thickness, h_c, at all points of a glacier:

$$h_c \leq \tau/\rho g h(\sin\alpha)F \leq 50\text{kPa}/(910 \text{ Kg m}^{-3})(9.81 \text{ m s}^{-2})(\sin\alpha)F \leq (5.6 \text{ m})/(\sin\alpha)F \qquad \text{(eqn. 2)}$$

To use this equation we need to know the ice surface and bedrock elevation at every point on a glacier (ice surface - bedrock = glacier thickness). Schilling and Hollin (1981) developed the following iterative solution:

$$e_{i+1} = e_i + (\tau/\rho g F)(\Delta x/h_i) \qquad \text{(eqn. 3)}$$

where e_i and e_{i+1} are ice-surface elevations at steps x_i and x_{i+1} back from the terminus of the glacier, Δx is the step length (500m) and h_i is the thickness at step x_i. If the critical thickness is reached at any point along the glacier, flow to downstream ice will be cut off leaving a block of unnourished stagnant ice. The active margin instantly retreats to the point where the critical thickness was reached.

The critical thickness component of the model tests to see if any or all of the following topographic variables are important controls of ice stagnation by inducing the ice to thin to the critical thickness: (1) longitudinal valley steps; (2) bedrock obstructions transverse to ice-flow direction; (3) variations in valley width; and (4) valley sinuosity causing variations in valley width.

Stagnation from ablation and active margin retreat rates

Stagnant ice can also be produced at the margin of a glacier if the rate of downward melting is slower than the active margin retreat rate (Figure 3b). The following equation was derived to determine the active margin retreat rate, dx/dt, using a 65-35% split of accumulation and ablation areas on either side of the equilibrium-line altitude (ELA) and a constant ELA rise rate, dy/dt:

$$dx/dt = (dy/dt)(dx/dy)[(1/2)(z_a/z_b) + 1] \qquad \text{(eqn. 4)}$$

where dx/dy is the slope at the ELA and z_a and z_b are valley widths at the downstream ends of the accumulation and ablation areas.

The active margin retreat rate can be used to calculate elapsed time between retreat steps (Δx) of the glacier. Ice stranded beyond the active margin during this jump is subjected to ablation over the calculated time. Ablation rate is controlled by slope angle and aspect of the ice surface at all points along the glacier. Insulating superglacial debris and shading topography could easily be incorporated into the model at this point; however, calculating reduction in ablation rate from these variables is complex. Other variables included in the model are the ELA rise rate and the bedrock slope at the ELA.

The two scenarios of ice stagnation are combined in a computer program written to evaluate data from the fifty valleys examined in the aerial photo survey (Figure 4). Results from this program are not yet available.

REFERENCES CITED

Atwood, W. and Mather, K., 1932. Physiography and Quaternary Geology of the San Juan Mountains, Colorado. USGS Professional Paper 166.

Flint, R.F., 1971. Glacial and Quaternary Geology. John Wiley and Sons, Inc. p 892.

Glen, J.W., 1954. The creep of polycrystalline ice. Proceedings of the Royal Society of London, A, 228: 519-538.

Nye, J.F., 1965. The flow of a glacier in a channel of rectangular, elliptic or parabolic cross-section:. Journal of Glaciology, v. 6, p. 695-715.

Schilling, David. H. and Hollin, John, T., 1981. Numerical reconstructions of valley glaciers and small ice caps, *in* Denton, G.H. and Hughes, T.J., *eds.*, The last great ice sheets. John Wiley and Sons, New York, p. 484.

Figure 3a

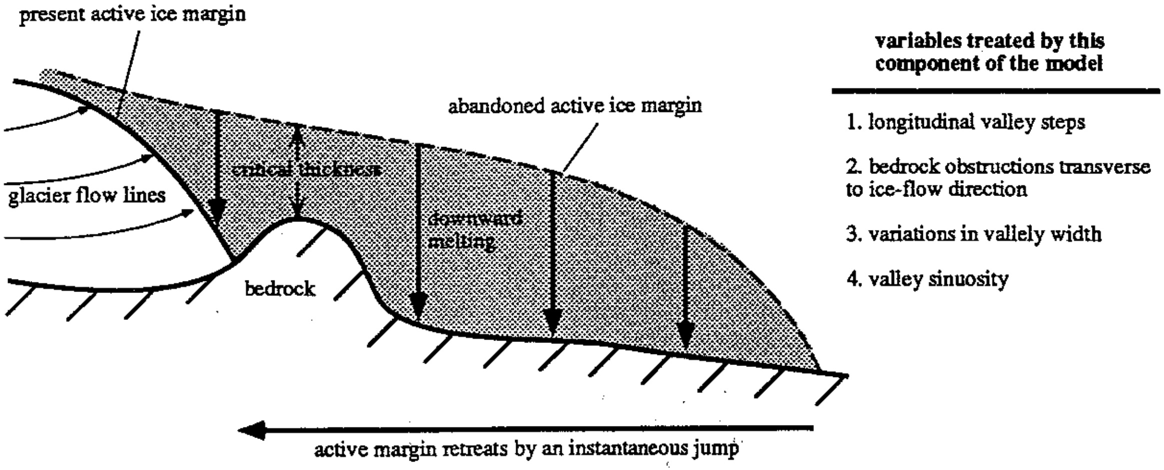

Figure 3b

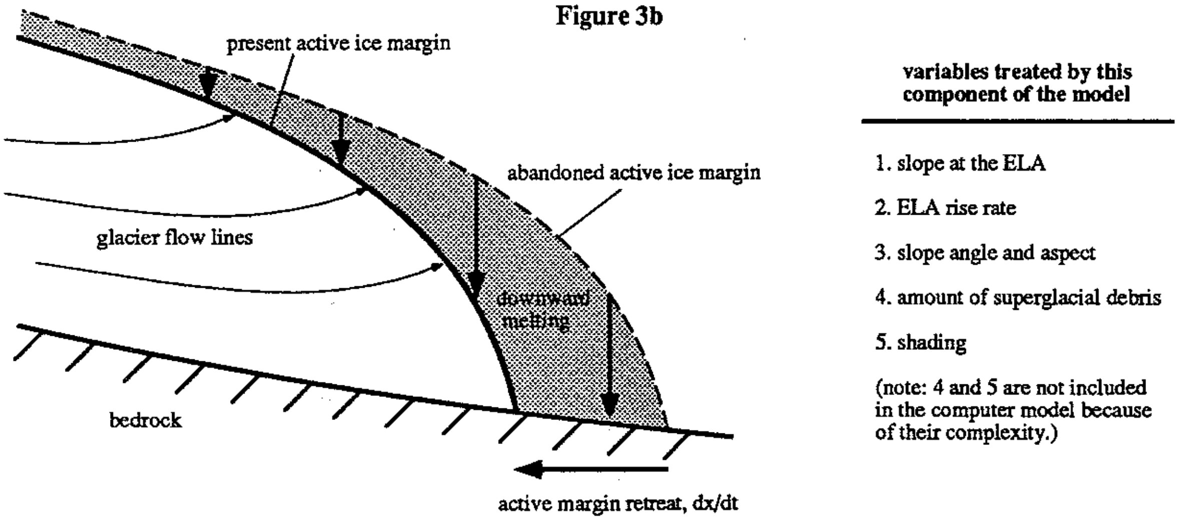

Figure 3. Two scenarios for ice stagnation. Shaded areas indicate ice stranded beyond the active margin which is subjected to downward melting. **3a)** Ice stagnation from topographically induced thinning to the critical thickness and **3b)** ice stagnation from slower downward melting than active ice margin retreat.

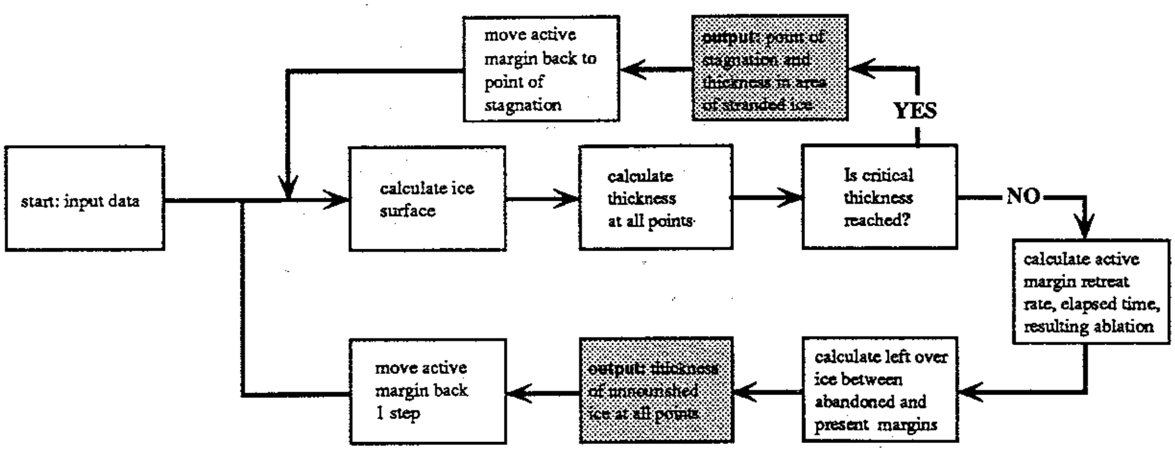

Figure 4. Flow chart for ice stagnation computer model. Shaded boxes indicate steps where output is produced.

PLEISTOCENE, HOLOCENE, AND MODERN CARBONATE SYSTEMS, BAHAMAS

FACULTY

H. Allen Curran, Smith College
Benjamin J. Greenstein, Smith College
Brian White, Smith College
Mark A. Wilson, The College of Wooster

STUDENTS

Rebecca Beavers, Williams College
Kathryn Desmarais, Beloit College
Nicole Fraser, Smith College
Lisa Greer, Colorado College
Julia L. Hohman, The College of Wooster
Susan P. Jennings, Trinity University
Heather A. Moffat, Smith College
Kathryn Michel Riesenberg, Colorado College
Durelle Smith, Smith College
Whitney L. Swift, Washington & Lee University

VISITORS

Carol Mankiewicz, Beloit College
Odell McGuire, Washington & Lee University
Carl Mendelson, Beloit College
Paul Myrow, Colorado College
Perry Roehl, Trinity University

PROJECT ASSISTANT

David White, Vassar College ('92)